Inorg. Chem. **2003**, *42*, 5594–5603

Binuclear Copper(II) Complexes of Xylyl-Bridged Bis(1,4,7-triazacyclononane) Ligands

Fiona H. Fry,[†] Leone Spiccia,*[,†] Paul Jensen,[†] Boujemaa Moubaraki,[†] Keith S. Murray,[†] and Edward R. T. Tiekink[‡]

School of Chemistry, P.O. Box 23, Monash University, Victoria 3800, Australia, and Department of Chemistry, The University of Adelaide, Australia 5005

Received March 10, 2003

Copper(II) complexes of three bis(tacn) ligands, $[Cu_2(T_2\text{-}o\text{-}X)Cl_4]$ (**1**), $[Cu_2(T_2\text{-}m\text{-}X)(H_2O)_4](ClO_4)_4\cdot H_2O\cdot NaClO_4$ (**2**), and $[Cu_2(T_2\text{-}p\text{-}X)Cl_4]$ (**3**), were prepared by reacting a Cu(II) salt and L·6HCl (2:1 ratio) in neutral aqueous solution [T_2-*o*-X = 1,2-bis(1,4,7-triazacyclonon-1-ylmethyl)benzene; T_2-*m*-X = 1,3-bis(1,4,7-triazacyclonon-1-ylmethyl)benzene; T_2-*p*-X = 1,4-bis(1,4,7-triazacyclonon-1-ylmethyl)benzene]. Crystals of $[Cu_2(T_2\text{-}m\text{-}X)(NPP)(\mu\text{-}OH)](ClO_4)\cdot H_2O$ (**4**) formed at pH = 7.4 in a solution containing **2** and disodium 4-nitrophenyl phosphate (Na_2NPP). The binuclear complexes $[Cu_2(T_2\text{-}o\text{-}XAc_2)(H_2O)_2](ClO_4)_2\cdot 4H_2O$ (**5**) and $[Cu_2(T_2\text{-}m\text{-}XAc_2)(H_2O)_2](ClO_4)_2\cdot 4H_2O$ (**6**) were obtained on addition of $Cu(ClO_4)_2\cdot 6H_2O$ to aqueous solutions of the bis(tetradentate) ligands T_2-*o*-XAc_2 (1,2-bis((4-(carboxymethyl)-1,4,7-triazacyclonon-1-yl)methyl)benzene and T_2-*m*-XAc_2 (1,3-bis((4-(carboxymethyl)-1,4,7-triazacyclonon-1-yl)methyl)-benzene), respectively. In the binuclear complex, **3**, three N donors from one macrocycle and two chlorides occupy the distorted square pyramidal Cu(II) coordination sphere. The complex features a long Cu···Cu separation (11.81 Å) and intermolecular interactions that give rise to weak intermolecular antiferromagnetic coupling between Cu(II) centers. Complex **4** contains binuclear cations with a single hydroxo and *p*-nitrophenyl phosphate bridging two Cu(II) centers (Cu···Cu = 3.565(2) Å). Magnetic susceptibility studies indicated the presence of strong antiferromagnetic interactions between the metal centers ($J = -275$ cm^{-1}). Measurements of the rate of BNPP (bis(*p*-nitrophenyl) phosphate) hydrolysis by a number of these metal complexes revealed the greatest rate of cleavage for $[Cu_2(T_2\text{-}o\text{-}X)(OH_2)_4]^{4+}$ ($k = 5 \times 10^{-6}$ s^{-1} at pH = 7.4 and $T = 50$ °C). Notably, the mononuclear $[Cu(Me_3tacn)(OH_2)_2]^{2+}$ complex induces a much faster rate of cleavage ($k = 6 \times 10^{-5}$ s^{-1} under the same conditions).

Introduction

The coordination chemistry of the small tridentate macrocycle 1,4,7-triazacyclononane (tacn) has attracted interest for a number of decades. Determinations of the crystal structures of two copper(II) complexes, $[Cu(tacn)Br_2]$[1] and $[Cu(tacn)Cl_2]$,[2] ascertained that the 5-coordinate Cu(II) centers in these complexes adopt square pyramidal (SP) geometries, with one nitrogen occupying the apical site and the other two lying in the basal plane. This is indeed a feature of 5-coordinate Cu(II) complexes of tacn derivatives.[3−6] Subsequent reports of the $[Cu(tacn)_2]^{2+}$ complex confirmed that two tacn rings can also sandwich one Cu(II) center such that the metal center resides in a distorted octahedral environment due to Jahn−Teller distortion.[7,8] Since these early studies, this small tridentate macrocycle and its

* To whom correspondence should be addressed. E-mail: leone.spiccia@sci.monash.edu.au. Fax: +61 3 9905 4597.

† Monash University.

‡ The University of Adelaide. Present address: Department of Chemistry, The National University of Singapore, Singapore 117543.

(1) Bereman, R. D.; Churchill, M. R.; Schaber, P. M.; Winkler, M. E. *Inorg. Chem.* **1979**, *18*, 3123.

(2) Schwindinger, W. F.; Fawcett, T. G.; Lalancette, R. A.; Potenza, J. A.; Schugar, H. J. *Inorg. Chem.* **1980**, *19*, 1379.

(3) Graham, B.; Fallon, G. D.; Hearn, M. T. W.; Hockless, D. C. R.; Lazarev, G.; Spiccia, L. *Inorg. Chem.* **1997**, *36*, 6366.

(4) Brudenell, S. J.; Spiccia, L.; Tiekink, E. R. T. *Inorg. Chem.* **1996**, *35*, 1974. (b) Brudenell, S. J.; Spiccia, L.; Bond, A. M.; Comba, P.; Hockless, D. C. R. *Inorg. Chem.* **1998**, *37*, 3705.

(5) DasGupta, B.; Katz, C.; Israel, T.; Watson, M.; Zompa, L. J. *Inorg. Chim. Acta* **1999**, *292*, 172.

(6) Blake, A. J.; Fallis, I. A.; Gould, R. O.; Parsons, S.; Ross, S. A.; Schröder, M. *J. Chem. Soc., Chem. Commun.* **1994**, 2467.

(7) Chaudhuri, P.; Oder, K.; Weighardt, K.; Weiss, J.; Reedjik, J.; Hinrichs, W.; Wood, J.; Ozarowski, A. M.; Stratemaier, H.; Reinen, D. *Inorg. Chem.* **1986**, *25*, 2951.

(8) Beveridge, A. D.; Lavery, A. J.; Walkinshaw, M. D.; Schröder, M. *J. Chem. Soc., Dalton Trans.* **1987**, 373.

10.1021/ic0342595 CCC: $25.00 © 2003 American Chemical Society
Published on Web 08/08/2003

derivatives have been used in the development of, for example, model compounds for the active sites of enzymes,[9−13] catalytic agents for organic transformations,[14,15] photoactive materials,[16,17] and protein purification methods.[18] A number of these applications rely on the high thermodynamic stability of tacn complexes (for Cu(II) log $K_f = 15.5$).[19]

Investigations have also focused on the coordination chemistry of assemblies consisting of two or more tacn macrocycles connected via organic backbones.[5,20−22] Such ligands and *N*-alkyl and *N*-benzyl derivatives thereof have been used in the synthesis of mononuclear and polynuclear metal complexes with novel structural, electronic, and functional properties, applicable, for example, in biomimetic studies and in the study of magnetic exchange interactions in polynuclear metal complexes.[5,20−24] The introduction of pendant coordinating groups, usually through N-functionalization with alcohols, amines, carboxylates, imidazoles, phosphonates, pyridyls, etc., enabled systematic variation of the environment that the ligand provides to the metal center.[3−5,11,20−22,25,26]

In comparison with alkyl bridged ($n = 2-8$) $(tacn)_2$ ligands, the coordination chemistry of $(tacn)_n$ assemblies with aromatic linkers has been less intensely studied, but complexes of ligands with naphthalene,[27] xylene,[3,5,28] mesitylene,[11,29] and durene[30,31] have been reported. We report here the synthesis and characterization of Cu((II) complexes

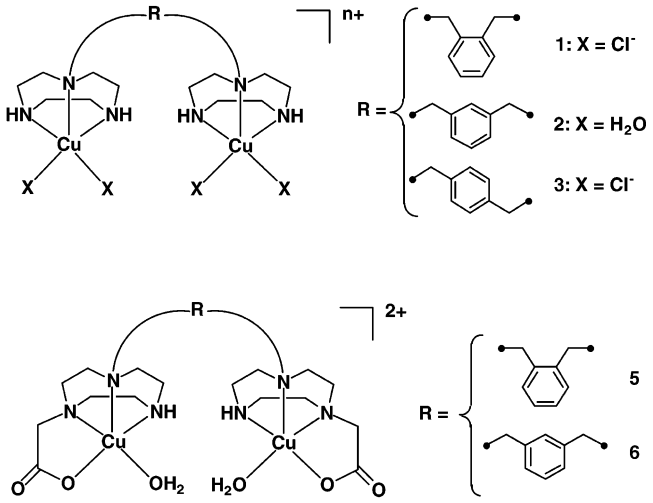

Figure 1. Complexes **1**−**3**, **5**, and **6**.

formed by xylyl-bridged $(tacn)_2$ ligands [1,2-bis(1,4,7-triazacyclonon-1-ylmethyl)benzene (T_2-*o*-X), 1,3-bis(1,4,7-triazacyclonon-1-ylmethyl)benzene (T_2-*m*-X), 1,4-bis(1,4,7-triazacyclonon-1-ylmethyl)benzene (T_2-*p*-X), 1,2-bis((4-(carboxymethyl)-1,4,7-triazacyclonon-1-yl)methyl)benzene (T_2-*o*-XAc_2), 1,3-bis((4-(carboxymethyl)-1,4,7-triazacyclonon-1-yl)methyl)benzene (T_2-*m*-XAc_2)]. In addition to the X-ray structures and variable-temperature magnetic studies of two of the complexes, $[Cu_2(T_2\text{-}p\text{-}X)Cl_4]$ (**3**) and $[Cu_2(T_2\text{-}m\text{-}X)(NPP)(\mu\text{-}OH)](ClO_4)\cdot H_2O$ (**4**), we report the rate constants for the cleavage of BNPP by a selection of these Cu(II) complexes.

Results and Discussion

Synthesis of Complexes. The copper(II) complexes of T_2-*o*-X and T_2-*p*-X (Figure 1) were synthesized by addition of aqueous solutions of L·6HCl to 2 equiv of $CuCl_2$ in water and adjusting the pH to ca. 7. Workup gave crystals of $[Cu_2(T_2\text{-}o\text{-}X)Cl_4]$ (**1**) and $[Cu_2(T_2\text{-}p\text{-}X)Cl_4]$ (**3**), the latter being suitable for X-ray crystallography. In the case of the T_2-*m*-X complex, T_2-*m*-X·6HCl and cupric perchlorate were reacted in a 1:2 molar ratio to give the complex, which was purified by cation exchange chromatography and isolated as $[Cu_2(T_2\text{-}m\text{-}X)(H_2O)_4](ClO_4)_4\cdot H_2O\cdot NaClO_4$ (**2**). Dark blue needles of $[Cu_2(T_2\text{-}m\text{-}X)(NPP)(\mu\text{-}OH)](ClO_4)\cdot H_2O$ **(4)** precipitated when a neutral solution containing **2** and disodium 4-nitrophenyl phosphate (Na_2NPP) was allowed to stand overnight at 38 °C (pH ∼ 7.4 maintained by a HEPES buffer). The IR spectra of these complexes show sharp bands due to the NH stretches of the secondary amines of the tacn rings in the 3200−3350 cm^{-1} region. The fingerprint region shows bands due to stretching vibrations of the aromatic groups connecting the tacn macrocycles. In the case of **4**, stretching vibrations of the bridging hydroxide and the water of crystallization were observed at 3458 and 3577 cm^{-1}, while **2** exhibited a broad OH stretch at 3420 cm^{-1}. The

(9) Halfen, J. A.; Jazdzewski, B. A.; Mahapatra, S.; Berreau, L. M.; Wilkinson, E. C.; Que, L., Jr.; Tolman, W. B. *J. Am. Chem. Soc.* **1997**, *119*, 8217.
(10) McCue, K. P.; Voss, D. A.; Jr, Marks, C.; Morrow, J. R. *J. Chem. Soc., Dalton Trans.* **1998**, 2961. (b) McCue, K. P.; Morrow, J. R. *Inorg. Chem.* **1999**, *38*, 6136.
(11) Spiccia, L.; Graham, B.; Hearn, M. T. W.; Lazarev, G.; Moubaraki, B.; Murray, K. S.; Tiekink, E. R. T. *J. Chem. Soc., Dalton Trans.* **1997**, 4089.
(12) Adams, H.; Bailey, N. A.; Dwyer, M. J. S.; Fenton, D. E.; Hellier, P. C.; Hempstead, P. D.; Latour, J. M. *J. Chem. Soc., Dalton Trans.* **1993**, 1207.
(13) Kövári, E.; Krämer, R. *J. Am. Chem. Soc.* **1996**, *118*, 12704.
(14) De Vos, D.; Meinershagen, J. L.; Bein, T. *Angew. Chem., Int. Ed. Engl.* **1996**, *35*, 2211. Zondervan, C.; Hage, R.; Feringa, B. L. *Chem. Commun.* **1997**, 419.
(15) Berkessel, A.; Sklorz, C. A. *Tetrahedron Lett.* **1999**, *40*, 7965.
(16) Sun, L.; Hammarström, L.; Akermark, B.; Styring, S. *Chem. Soc. Rev.* **2001**, *30*, 36.
(17) Burdinski, D.; Bothe, E.; Wieghardt, K. *Inorg. Chem.* **2000**, *39*, 105.
(18) Jiang, W.; Graham, B.; Spiccia, L.; Hearn, M. T. W. *J. Anal. Biochem.* **1998**, *255*, 47.
(19) Yang, R.; Zompa, L. J. *Inorg. Chem.* **1976**, *15*, 1499.
(20) Weighardt, K.; Tolksdorf, I.; Herrmann, W. *Inorg. Chem.* **1985**, *24*, 1230.
(21) Haidar, R.; Ipek, M.; DasGupta, B.; Yousaf, M.; Zompa, L. J. *Inorg. Chem.* **1997**, *36*, 3125.
(22) Zhang, X.; Hseih, W.-Y.; Margulis, T. N.; Zompa, L. J. *Inorg. Chem.* **1995**, *34*, 2883.
(23) Tolman, W. B. *Acc. Chem. Res.* **1997**, *30*, 227.
(24) Hegg, E. L.; Burstyn, J. N. *Coord. Chem. Rev.* **1998**, *173*, 133 and references therein.
(25) Blake, A. J.; Donlevy, T. M.; England, P. A.; Fallis, I. A.; Parsons, S.; Ross, S. A.; Schröder, M. *J. Chem. Soc., Chem. Commun.* **1994**, 1981. (b) Blake, A. J.; Danks, J. P.; Li, W.-S.; Lippolis, V.; Schröder, M. *J. Chem. Soc., Dalton Trans.* **2000**, 3034.
(26) Fry, F. H.; Graham, B.; Spiccia, L.; Hockless, D. C. R.; Tiekink, E. R. T. *J. Chem. Soc., Dalton Trans.* **1997**, 827.
(27) Young, M. J.; Chin, J. *J. Am. Chem. Soc.* **1995**, *117*, 10577.
(28) Farrugia, L. J.; Lovatt, P. A.; Peacock, R. D. *J. Chem. Soc., Dalton Trans.* **1997**, 911.
(29) Graham, B.; Spiccia, L.; Fallon, G. D.; Hearn, M. T. W.; Mabbs, F. E.; Moubaraki, B.; Murray, K. S. *J. Chem. Soc., Dalton Trans.* **2002**, 1226.
(30) Graham, B.; Grannas, M. J.; Hearn, M. T. W.; Kepert, C. M.; Spiccia, L.; Skelton, B. W.; White, A. H. *Inorg. Chem.* **2000**, *39*, 1092.
(31) Graham, B.; Hearn, M. T. W.; Junk, P. C.; Kepert, C. M.; Mabbs, F. E.; Moubaraki, B.; Murray, K. S.; Spiccia, L. *Inorg. Chem.* **2001**, *40*, 1536.

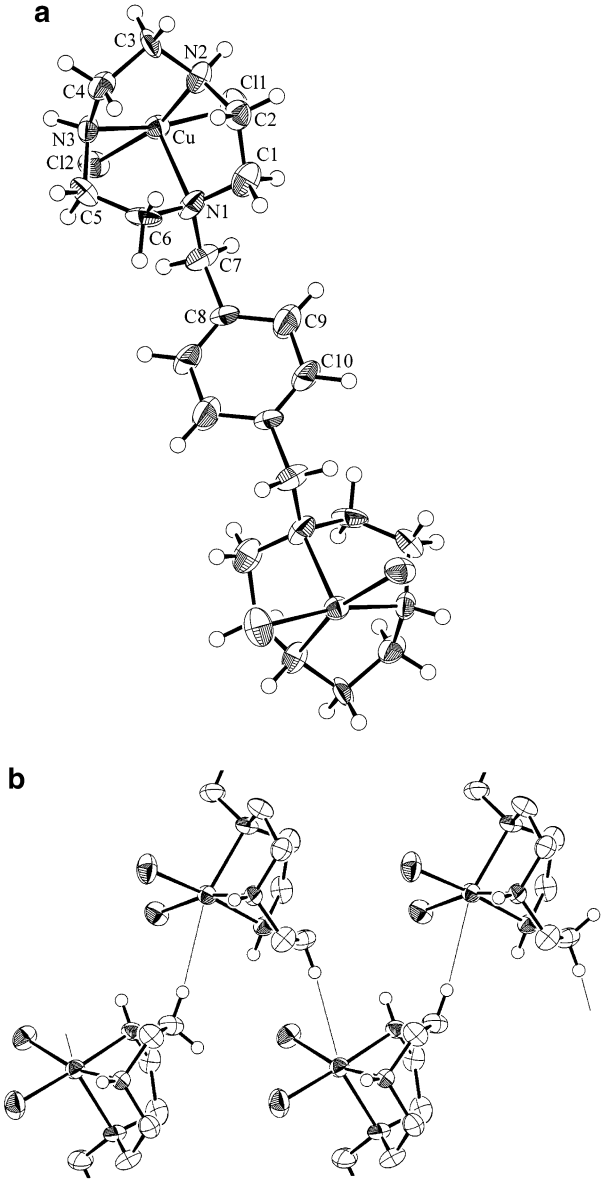

Figure 2. (a) ORTEP plot of $[Cu_2(T_2\text{-}p\text{-}X)Cl_4]$ (**3**) with atomic labeling scheme drawn at the 50% probability level. (b) Partial molecular packing diagram of $[Cu_2(T_2\text{-}p\text{-}X)Cl_4]$ (**3**) showing the interactions between molecules.

stretching vibrations of the phosphate moiety in **4** are masked by a strong perchlorate stretch at 1098 cm^{-1}. The asymmetric and symmetric stretches of the nitro group on the phosphate moiety can, however, be seen at 1518 and 1345 cm^{-1}. The analytical and spectroscopic data for all the complexes supported the proposed compositions.

Addition of 2 molar equiv of $Cu(ClO_4)_2 \cdot 6H_2O$ to aqueous solutions of the crude oils of T_2-*o*-X Ac_2 or T_2-*m*-X Ac_2 and adjustment of the pH to ca. 5 produced dark blue solutions which, following purification by cation exchange chromatography and concentration, yielded blue powders of complexes with elemental compositions corresponding to $[Cu_2(T_2\text{-}o\text{-}X\ Ac_2)(H_2O)_2](ClO_4)_2 \cdot 4H_2O$ (**5**) and $[Cu_2(T_2\text{-}m\text{-}X\ Ac_2)(H_2O)_2](ClO_4)_2 \cdot 4H_2O$ (**6**). The IR spectra of the complexes are virtually identical. Sharp NH stretches were observed at 3297 and 3316 cm^{-1}, respectively. Strong bands at 1598 (**5**) and 1624 (**6**) cm^{-1} and weaker bands at 1370 (**5**) and 1373 (**6**) cm^{-1} are assigned to the asymmetric and symmetric stretching modes of carboxylate groups, respectively, binding to Cu(II) in a unidentate fashion.[32] As expected, the electrospray mass spectra of the two compounds were very similar. In particular both spectra show a peak at *m*/*z* 701, which corresponds to the $\{[Cu_2(T_2\text{-}(o,m)\text{-}X\ Ac_2)]ClO_4\}^+$ ion.

Table 1. Comparison of Geometric Features of $[Cu_2(T_2\text{-}p\text{-}X)Cl_4]$ (**3**) with Those of Other Cu−tacn−Chloro Complexes

	3	$[Cu(tacn)Cl_2]$[2]	$[Cu_2(T_2\text{-but})Cl_4]$[22]
	Bond Lengths (Å)		
Cu−N(apical)	2.250(9)	2.246(4)	2.285(3)
Cu−N(basal)	2.02(1)	2.038(4)	2.034(4)
	2.046(9)	2.063(4)	2.061(4)
Cu−Cl	2.270(4)	2.268(1)	2.26(1)
	2.284(4)	2.312(1)	2.301(1)
	Bond Angles (deg)		
N(apical)−Cu−N(basal)	82.9(4)	83.0(2)	81.9(1)
	82.7(3)	82.6(2)	82.4(1)
N(basal)−Cu−N(basal)	83.5(4)	82.2(2)	82.9(1)
N(apical)−Cu−Cl	102.9(3)	105.8(1)	100.4(1)
	108.4(3)	107.2(1)	113.5(1)
N(basal)−Cu−Cl	89.4(3)	90.5(1)	88.3(1)
	90.2(3)	91.0(1)	91.5(1)
	166.3(2)	167.0(1)	161.1(1)
	170.4(3)	168.2(1)	173.3(1)

Crystal Structure of $[Cu_2(T_2\text{-}p\text{-}X)Cl_4]$ (3). The crystal structure of **3** has been determined but not to a high level of precision. Nevertheless, the molecular connectivity and crystal packing arrangement has been determined unambiguously. The complex is binuclear as shown in Figure 2a, and selected bond lengths and angles are shown in Table 1. The complex is centrosymmetric about the center of the xylyl aromatic ring, and the Cu(II) centers adopt an *anti*-conformation that gives rise to a large Cu···Cu separation of 11.81 Å. The Cu(II) center is in a distorted square pyramidal (SP) environment, with the basal plane defined by the two Cl atoms, Cl(1) and Cl(2), and the two secondary nitrogens, N(2) and N(3), while the apical site is occupied by the bridgehead nitrogen, N(1). The mean deviation of Cl(1), Cl(2), N(2), and N(3) from their least-squares plane is 0.045 Å, and the Cu(II) center lies 0.188(1) Å above this plane, toward N(1). The Cu−Cl distances of 2.270(4) and 2.284(4) Å are typical for such coordinations.[2] The Cu−N(equatorial) distances (2.02(1) and 2.046(9) Å) are shorter than the Cu−N(apical) distance (2.250(9) Å) as is expected for d^9 Cu(II) centers in SP geometry.[1−5] A τ value of 0.07, defined according Addison et al.,[33] indicates that the geometry is close to SP. Table 1 highlights that these features are also common to $[Cu(tacn)Cl_2]$[2] and polynuclear tacn complexes, such as $[Cu_2(T_2\text{-prop})Cl_4] \cdot 2H_2O$ (T_2-prop = 1,3-bis(1,4,7-triazacyclonon-1-yl)propane) and $[Cu_2(T_2\text{-but})Cl_4]$ (T_2-but = 1,3-bis(1,4,7-triazacyclonon-1-yl)butane).[22]

Figure 2b shows that there are some associations between the complex molecules. An interesting feature of the crystal structure is the alignment of hydrogen atoms to neighboring Cu(II) centers. These are most probably a consequence of

(32) Deacon, G. B.; Huber, F. *Inorg. Chim. Acta* **1985**, *104*, 41.
(33) Addison, A. W.; Rao, T. N.; Reedijk, J.; van Rijn, J.; Verschoor, G. C. *J. Chem. Soc., Dalton Trans.* **1984**, 1349.

N−H···Cl and C−H···Cl interactions as detailed below and give rise to weak intermolecular antiferromagnetic interactions (see Magnetism). Thus, a hydrogen attached to C(4) is separated from a symmetry-related Cu(II) center (symmetry operation: x, $^3/_2 - y$, $-^1/_2 + z$) by 2.75 Å. The C(4)···Cu distance is 3.719(11) Å, and the angle subtended at H is 175°. These interactions form a zigzag pattern within the crystal lattice. Each binuclear complex associates with two of these H atoms from neighboring complexes and also donates to another two complexes which are translated by one unit along the *c* axis from those complexes that donate to it. Therefore, each complex is involved in two acceptor and two donor interactions. The zigzag chains are reinforced by weak N−H···Cl and C−H···Cl interactions: N(3)−H···Cl(2) is 2.60 Å and N(3)···Cl(2) is 3.380(11) Å with the bonds centered about H at 139° (symmetry operation: x, $^3/_2 - y$, $^1/_2 + z$). These interactions link the molecules together in the same way as the associations mentioned above. Molecules related by translation along the *c* axis are linked together by C−H···Cl interactions [distances C(2)−H···Cl(1) 2.73 Å and C(2)···Cl(1) 3.705(10) Å and the angle about the H is 176° (symmetry operation: x, y, $1 + z$); distances C(4)−H···Cl(1) 2.78 Å and C(4)···Cl(1) 3.688(14) Å and the angle about the H is 156° (symmetry operation: x, y, $1 + z$)]. These associations described above generate a corrugated layer structure, stacked along the *a* axis. The links between the layers are provided by interactions between N(2)−H···Cl(2) [distances N(2)−H···Cl(2) 2.50 Å and N(2)···Cl(2) 3.293(12) Å, so that the angle about the H atom is 141° (symmetry operation: $^1/_2 + x$, y, $^1/_2 - z$)]. The crystal structure of the monohydrate derivative of **3** has been determined independently.[34] The two complexes are therefore psuedopolymorphic. In the hydrate, the oxygen atom is 3.42 Å from the Cu atom, and as such, the interesting Cu···H "contacts" observed in anhydrous form of **3** are not featured in the monohydrate.

Crystal Structure of [Cu$_2$(T$_2$-*m*-X)(NPP)(μ-OH)](ClO$_4$)·H$_2$O (4). The ORTEP diagram of the [Cu$_2$(T$_2$-*m*-X)(NPP)(μ-OH)]$^+$ cation (Figure 3a) clearly shows that the NPP^{2-} anion bridges two Cu(II) centers via two phosphate oxygens. A hydroxide bridge provides a further connection between the two metal centers. Selected bond distances and angles for the binuclear cation, showing the distortion from SP geometry for Cu(II) and the differences between the two unique metal centers, are given in Table 2. The corresponding bond lengths are very similar for Cu(1) and Cu(2); however, more significant variation in some of the corresponding bond angles about the two metal centers is apparent.

Adjacent cations in the structure are connected via hydrogen bonding as detailed in Table 3 and Figure 3b. The bridging hydroxide, O(1), and amines, N(3) and N(6), donate their protons to the uncoordinated phosphate oxygen, O(5A), of an adjacent cation [O(1)···O(5A) = 2.783(4) Å, N(3)···O(5A) = 2.898(4) Å, and N(6)···O(5A) = 2.957(5) Å]. These intercation hydrogen bonds give linear chains propagating in the *b* direction (Figure 3b). The lattice water and perchlorate anions are also involved in hydrogen bonding. The water molecule, O(8), donates one proton to phosphate oxygen, O(5), and the other to perchlorate oxygen, O(9), which in turn also accepts another hydrogen bond from an amine, N(2), of an adjacent tacn moiety [O(8)···O(5) = 2.794(5) Å, O(8)···O(9) = 2.831(6) Å, and N(2)···O(9) = 2.946(6) Å]. These interactions effectively result in intracation connections via the three hydrogen bonds (Figure 3b). C−H···O contacts also exist within the structure of **4**. The strongest of these is between a phenyl proton on the NPP

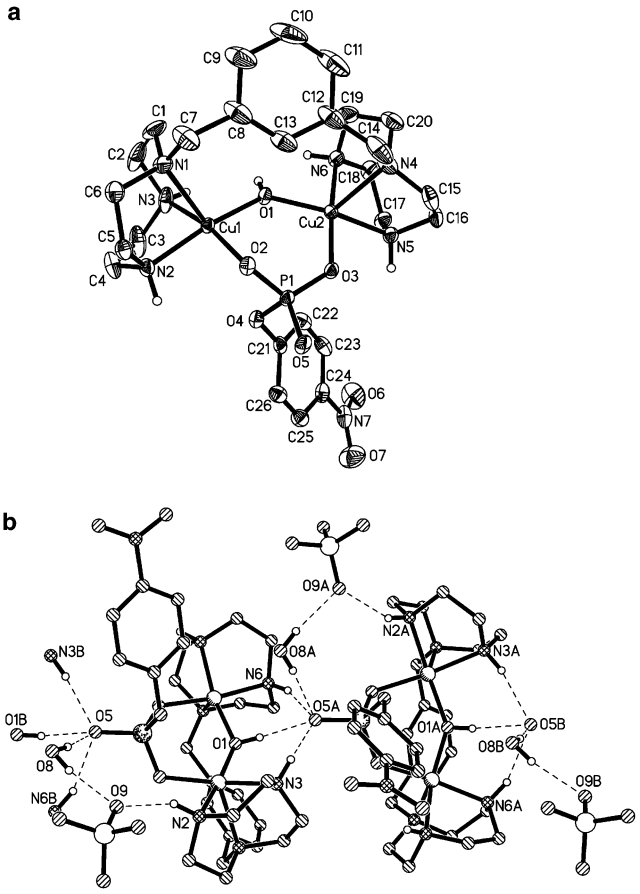

Figure 3. (a) ORTEP plot of the [Cu$_2$(T$_2$-*m*-X)(NPP)(μ-OH)]$^+$ cation of **4** drawn at the 50% probability level with atomic labeling scheme. (b) Extended packing array of **4** showing the H-bonded chains formed within the crystal.

Table 2. Selected Bond Distances (Å) and Angles (deg) for **4**

Cu(1)−N(1)	2.318(3)	Cu(2)−N(4)	2.312(4)
Cu(1)−N(2)	2.025(3)	Cu(2)−N(5)	2.047(3)
Cu(1)−N(3)	2.030(3)	Cu(2)−N(6)	2.028(3)
Cu(1)−O(1)	1.903(2)	Cu(2)−O(1)	1.912(2)
Cu(1)−O(2)	1.967(2)	Cu(2)−O(3)	1.951(3)
O(2)−P(1)−O(3)	115.6(2)	O(3)−P(1)−O(4)	107.2(2)
O(2)−P(1)−O(4)	101.8(2)	O(3)−P(1)−O(5)	111.8(2)
O(2)−P(1)−O(5)	113.1(2)	O(4)−P(1)−O(5)	106.2(2)
N(1)−Cu(1)−N(2)	82.1(2)	N(4)−Cu(2)−N(5)	82.6(2)
N(1)−Cu(1)−N(3)	81.9(2)	N(4)−Cu(2)−N(6)	82.6(2)
N(1)−Cu(1)−O(1)	108.7(2)	N(4)−Cu(2)−O(1)	113.2(2)
N(1)−Cu(1)−O(2)	106.5(2)	N(4)−Cu(2)−O(3)	98.3(2)
N(2)−Cu(1)−N(3)	83.7(2)	N(5)−Cu(2)−N(6)	83.1(2)
N(2)−Cu(1)−O(1)	168.3(2)	N(5)−Cu(2)−O(1)	162.7(2)
N(2)−Cu(1)−O(2)	89.1(2)	N(5)−Cu(2)−O(3)	90.2(1)
N(3)−Cu(1)−O(1)	93.1(2)	N(6)−Cu(2)−O(1)	91.7(1)
N(3)−Cu(1)−O(2)	168.1(2)	N(6)−Cu(2)−O(3)	173.1(2)
O(1)−Cu(1)−O(2)	92.2(2)	O(1)−Cu(2)−O(3)	94.2(1)
Cu(1)−O(1)−Cu(2)	138.3(2)		

(34) Wang, H.-J.; Wu, C.-T.; Luo, B.-S. *Jiegou Huaxue* **1998**, *17*, 119.

Table 3. Hydrogen Bond Distances (Å) and Angles (deg) for **4**

D−H···A	D−H	H···A	D···A	∠D−H···A
O(1)−H(1)···O(5)[a]	0.83	1.97	2.783(4)	168
N(3)−H(3)···O(5)[a]	0.93	2.02	2.898(4)	156
N(6)−H(6)···O(5)[a]	0.93	2.07	2.957(5)	159
O(8)−H(8A)···O(5)	0.85	1.95	2.794(5)	173
O(8)−H(8B)···O(9)	0.84	2.00	2.831(6)	169
N(2)−H(2)···O(9)	0.93	2.11	2.946(6)	150
C(22)−H(22)···O(8)[a]	0.95	2.38	3.081(5)	131
C(7)−H(7A)···O(7)[b]	0.99	2.52	3.211(7)	127
C(18)−H(18A)···O(6)[c]	0.99	2.55	3.042(5)	110

[a−c]Symmetry codes: (*a*) 1/2 − *x*, *y* − 1/2, z; (*b*) 1/2 − *x*, 1/2 − *y*, *z* − 1/2; (*c*) 1 − *x*, −*y*, 1 − *z*.

moiety and the water molecule [H(22)···O(8)* = 2.38 Å]. These effectively occur within the chains described above. Other C−H···O contacts between the nitro group on the NPP moiety and C−H protons on the T_2-*m*-X ligand connect the parallel linear chains in the *a* and *c* directions [H(7A)···O(7)* = 2.52 Å and H(18A)···O(6)* = 2.55 Å]. Full details are given in Table 3.

A comparison of the structure of **4** with the related structure reported by Graham et al.[11] is warranted since both complexes have two copper centers linked by a hydroxide and a phosphate moiety. Only slight structural differences are apparent. The Cu(1)···Cu(2) distance of 3.565(2) Å for **4** is identical with that of the related trinuclear cluster, with a Cu(1)···Cu(2) distance of 3.557(4) Å. The Cu(1)−O−Cu(2) angles of 138.3(2)° (for **4**) and 134.6(6)° also compare favorably. The presence of the phosphate bridge increases both the Cu···Cu distance as well as the Cu−O−Cu bond angle relative to systems with two single atom bridges. For comparison, the structure of $[Cu_2(T_2\text{-}m\text{-}X)(\mu\text{-}OH)_2]^{2+}$ reported by Farrugia et al.[28] shows a Cu(1)···Cu(2) distance of 2.95 Å and Cu(1)−O−Cu(2) angles of ca. 99.6°.

Structures have been reported in which two Cu(II) centers are bridged through an O−P−O bridge and an oxygen atom located on the ligand backbone rather than a hydroxo bridge.[35−37] In a Cu(II) complex of 2,6-bis[(bis(2-benzimidazolylmethyl)amino)methyl]-4-methylphenolate, reported by Wall et al.,[36] a dibenzyl phosphate bridge (O−P−O) between the two copper centers is further supported by an endogenous phenolate bridge. The Cu···Cu distance was found to be slightly longer at 3.670(4) Å; cf. 3.565(2) Å for **4**. The Cu(1)−O−Cu(2) angle spanned by the copper centers and the bridging phenolate oxygen was more acute (126.2°) than that in **4**. In the related complex of 2,6-bis[(bis(2-pyridylmethyl)amino)methyl]phenolate, reported by Karlin and coworkers,[35] the Cu···Cu distance is significantly larger at 3.773(4) Å, while Yamaguchi et al.[37] found that in a dinuclear Cu(II) complex of *N*,*N*,*N*′,*N*′-tetrakis{(6-methyl-2-pyridyl)-methyl}-1,3-diaminopropan-2-ol, with an endogenous oxygen bridge from the propanol ligand backbone linking the two copper(II) centers and an O−P−O bridge formed by BNPP, the Cu···Cu distance was 3.78 Å and the Cu−O−Cu bond angle was larger than that found in **4** at 140.2°. The Cu···Cu distance in **4** is shorter than the Zn···Zn separation of 3.94 Å found in phosphate-modified alkaline phosphatase (AP), where one O−P−O bridges two Zn centers,[38] and comparable to the shortest M···M distance in phosphate-modified phospholipase C (PLC), in which phosphate coordinates to all three zinc centers, giving distances of the following: Zn(1)···Zn(2) = 5.7 Å; Zn(1)···Zn(3) = 3.5 Å; Zn(2)···Zn(3) = 4.5 Å.[39] In PLC, however, the short Zn···Zn separation is a consequence of a single phosphate oxygen bridge.

Electronic Spectra. The aqueous solution electronic spectra of **1**−**3** exhibit two d → d absorption maxima (λ_{max}) at ca. 645 and 1040 nm which are typical of distorted SP copper(II) complexes formed by tacn-based ligands and are due to $d_{z^2} \rightarrow d_{x^2-y^2}$ and $d_{yz} \rightarrow d_{x^2-y^2}$ transitions of Cu(II) centers residing in such a geometry.[3,21,40] Cu(II) complexes with TBP geometry typically exhibit an absorption maximum ca. 800−900 nm.[41] The diffuse reflectance spectra compare well with the solution spectra with the exception of the spectrum of **4**, for which a 60 nm blue shift in the maximum for the reflectance spectrum indicates a solid-state geometry closer to SP.

Magnetic and ESR Properties. Room-temperature magnetic moments of **1**−**3**, **5**, and **6** are in the range normally expected for mononuclear or polynuclear copper(II) complexes with uncoupled or weakly coupled d^9 Cu(II) centers. Complex **4** shows a moment which is lower than the expected value due to antiferromagnetic coupling between the metal centers (see below).

Variable-temperature magnetic studies were carried out on powdered samples of complexes of **3**, **5**, and **6** over the temperature range 4.2−300 K. For **5** and **6** the χ_{Cu} values follow a Curie temperature dependence ($\chi_{Cu} = C/T$) indicative of little or no coupling between the Cu(II) centers. Complex **3** shows a decrease in μ_{eff} as the temperature decreases, which is indicative of weak antiferromagnetic coupling (Figure 4). The corresponding magnetic susceptibilities show a maximum at ca. 10 K. The data for **3** were fitted to a modified Bleaney−Bowers equation,[42] calculated for two $S = 1/2$ centers under a $-2JS_1 \cdot S_2$ spin Hamiltonian, using a nonlinear least-squares fitting routine. The susceptibility equation (eq 1) allows for a monomeric impurity seen commonly in such systems,[43] assuming the *g*-value is the same as the complex. All the symbols have their usual meaning, and *P* is the amount of monomeric impurity. The parameters obtained from the fit obtained were the following: *g* value = 1.99; $J = -8$ cm^{-1}; $P = 0.18$. The coupling

(35) Mahroof-Tahir, M.; Karlin, K. D.; Chen, Q.; Zubieta, J. *Inorg. Chim. Acta* **1993**, *207*, 135.
(36) Wall, M.; Humes, R. M.; Chin, J. *Angew. Chem., Int. Ed. Engl.* **1993**, *32*, 1633.
(37) Yamaguchi, K.; Akagi, F.; Fujinami, S.; Shionota, M.; Suzuki, S. *Chem. Commun.* **2001**, 375.
(38) Hansen, S.; Hansen, L. K.; Hough, E. *J. Mol. Biol.* **1992**, *255*, 543.
(39) Kim, E. E.; Wyckoff, H. W. *J. Mol. Biol.* **1991**, *218*, 449.
(40) McLachlan, G. A.; Fallon, G. D.; Martin, R. L.; Spiccia, L. *Inorg. Chem.* **1995**, *34*, 254.
(41) Hathaway, B. J. In *Comprehensive Coordination Chemistry*; Wilkinson, G., Gillard, R. D., McCleverty, J. A., Eds.; Pergamon: Oxford, U.K., 1987; Vol. 5, pp 533−774 and referenced therein.
(42) Bleaney, B.; Bowers, K. D. *Proc. R. Soc. London, Ser. A* **1952**, *214*, 451.
(43) Kruger, P. E.; Moubaraki, B.; Fallon, G. D.; Murray, K. S. *J. Chem. Soc., Dalton Trans.* **2000**, 713.

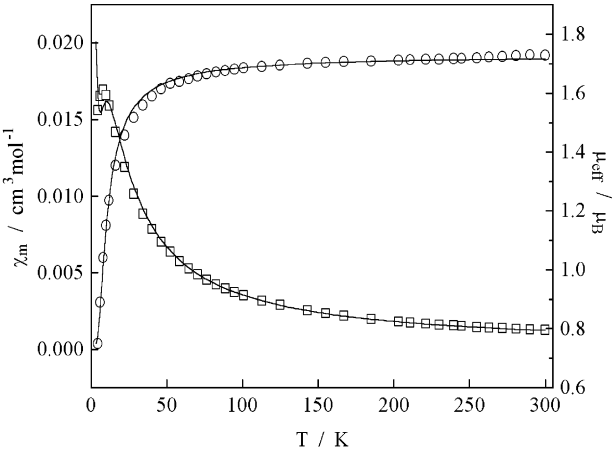

Figure 4. Plot of χ_m (□) and μ_{eff} (○) (per Cu) versus temperature for complex **3** showing the fitted data.

is unlikely to be intramolecular across the aromatic ring (Cu···Cu distance = 11.81 Å) but more likely to be intermolecular in nature and involving an H-bonded pathway between N(3) and Cl in an adjacent molecule (see Figure 2b).

$$\chi_{Cu} = \frac{Ng^2\beta^2}{kT}\left[3 + \exp\left(\frac{-2J}{kT}\right)\right]^{-1}(1 - P) + \frac{Ng^2\beta^2 P}{4kT} + N_\alpha \quad (1)$$

X-band ESR spectra of the complexes, recorded at 77 K for frozen solutions of 1:1 ethylene glycol/water for complexes **1**−**3** and DMF/toluene for complexes **5** and **6**, are shown in Figure 5. The complexes show a strong signal centered around 3000 G. The parameters obtained are typical of an SP environment around the Cu(II) center with $g_{\|} > g_{\perp} > 2$.[4b,40] Three of the expected four hyperfine signals are seen with the fourth hidden under the $g_{\perp}$ line. Additional hyperfine lines are seen in the spectra for **1** and **2**, which may be indicative of either different copper environments within the complexes, perhaps involving partial solvation, or of the existence of weak dipole−dipole coupling between the copper centers. Brudenell et al.[4b] have described the latter phenomena in binuclear copper−tacn complexes, with the former explanation ruled out through crystallographic analysis of the complexes. They reported that the increasing Cu···Cu separations, brought about by the increasing length of the bridge between two tacn units, decreased the dipole−dipole coupling between the copper centers. The complexes of the *ortho*- and *meta*-xylyl-bridged ligands described here showed additional hyperfine lines due to this dipole−dipole coupling. This phenomenon has also been documented in other studies of copper(II) complexes.[44] Weak half-field ($\Delta m_s = \pm 2$) lines would be predicted at ca. 1500 G if dipole−dipole coupling was operative.

Magnetic susceptibilities for **4** were measured in a field of 1 T over the temperature range of 300−4.2 K. The variable-temperature magnetic moment plot (Figure 6) shows a decrease in magnetic moment with temperature which is indicative of strong antiferromagnetic coupling between the copper(II) centers. The plot reaches a minimum value of 0.10

(44) Smith, T. D.; Pilbrow, J. R. *Coord. Chem. Rev.* **1974**, *13*, 173.

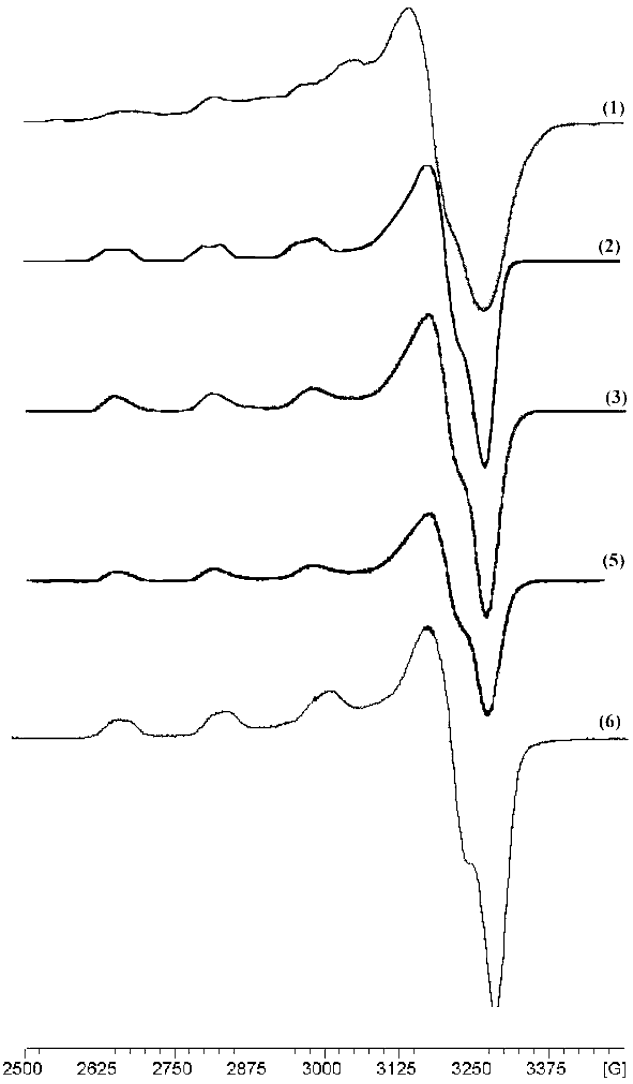

Figure 5. ESR spectra of complexes **1**−**3**, **5**, and **6** recorded at 77 K for frozen solutions of ethylene glycol/water (1:1) for **1**−**3** and DMF/toluene for **5** and **6**.

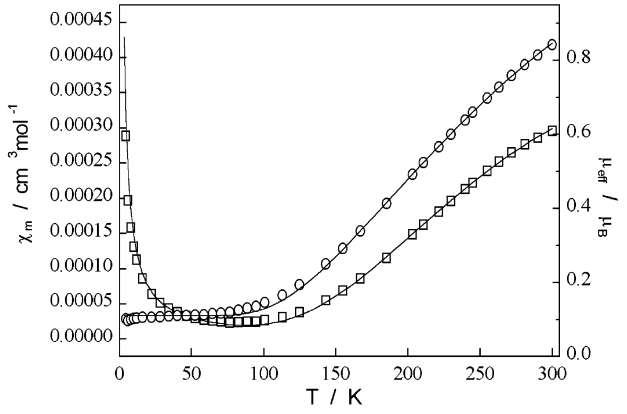

Figure 6. Plot of χ_m (□) and μ_{eff} (○) (per Cu) versus temperature for complex **4**.

μ_B at ca. 90 K, after which the magnetic moment is fairly constant. The increase in the corresponding magnetic susceptibility observed at low temperatures is due to a monomeric impurity.[43] The data were fitted to eq 1, and the parameters obtained are as follows: g value = 2.00; $J = -275$ cm^{-1}; $P = 0.004$. This large, negative value of J arises

primarily due to strong antiferromagnetic coupling across the Cu−O(H)−Cu bridge, since the NPP bridge and the *m*-xylyl moiety are poor superexchange pathways.[3] The OH link joins the Cu $d_{x^2-y^2}$ orbitals. The Cu···Cu distance of 3.57 Å and the Cu−O−Cu angle of 138.2° are predicted to lead to a *J* value of −515 cm^{-1} by use of Thompson's data[45] for single μ-OH-bridged complexes. This angular correlation, however, applies to a series of dinuclear compounds which contain an aromatic diazine (N−N) as the second bridge, and this does not allow for large Cu−O−Cu angles of the magnitude observed for **4**. It also has a superexchange ability different from that of the organophosphate, and so the angular correlation gives poor agreement with the present system, although strong antiferromagnetic coupling is anticipated, largely via the Cu−O(H)−Cu angle.

A more appropriate comparison is made with compounds such as $[(bpy)_2Cu(\mu\text{-}OH)(\mu\text{-}ClO_4)Cu(bpy)_2](ClO_4)_2$[46] for which *J* is −161 cm^{-1}, Cu−O−Cu = 141.6(3)°, and the Cu−Cu distance = 3.642(2) Å. Few [Cu(μ-OH)(μ-phosphate)Cu] bridged complexes are available for comparison. In a related trinuclear complex,[11] the [Cu(1)(OH)(O_2PO_2)-Cu(2)] moiety yielded $J_{12} = -161$ cm^{-1}, less than observed for **4**, even though the bridging geometry is rather similar. Clearly more examples of μ-OH, μ-phosphate bridged Cu(II) complexes are required.

The X-band ESR spectrum of **4**, recorded in a frozen DMF/toluene solution at 77 K, exhibits a very weak signal centered at ca. 3000 G ($g = 2.04$); however, the signal is most likely due to a monomeric impurity as seen in the magnetic susceptibility plot. This is not unexpected due to the strong coupling seen at low temperature in the magnetic susceptibility plot (Figure 5).

Phosphate Ester Hydrolysis. The ability of a selection of the binuclear copper(II) complexes to cleave phosphate esters was examined by measuring the rate of release of *p*-nitrophenylate from the phosphate diester, bis(4-nitrophenyl) phosphate (BNPP), under the same reaction conditions ([complex] = 1.7 mM, [BNPP] = 0.15 mM, pH = 7.4 (HEPES), and $T = 50$ °C). For the binuclear complexes and $[Cu(tacn)(H_2O)_2]^{2+}$, the rates for the hydrolysis of BNPP were calculated using the initial rates method routinely applied in the kinetic analysis of such slow reactions (see, for example, refs 47−49). In the case of [Cu(Me_3tacn)-$(H_2O)_2]^{2+}$, the consecutive release of two *p*-nitrophenylate ions was followed and rate constants for the two processes were determined by fitting the time-dependent increase in absorbance to a double exponential equation for consecutive first-order reactions. The data are presented in Table 4.

The rate data indicate that the binuclear Cu(II) complexes of the xylyl-bridged bis(tacn) ligands accelerate the rate of BNPP hydrolysis relative to the "parent" complex, [Cu(tacn)-$(H_2O)_2]^{2+}$. Remarkably, $[Cu_2T_2\text{-}o\text{-}X(H_2O)_4]^{4+}$ exhibits the fastest rate of BNPP hydrolysis. The rate is 25-fold faster than that for the parent tacn complex and 6-fold faster than that for the *m*-xylyl-bridged derivative. In other biomimetic studies applying these binucleating ligands, the Cu(II) complexes of the *m*- and *p*-xylyl analogues have proved more effective agents for cleaving GpppG, a model for the 5′-cap of mRNA, than the parent tacn complex, but the *o*-xylyl analogue was not examined.[10b] Unfortunately, the formation of a precipitate in the reaction mixtures prevented us from determining the rate of BNPP hydrolysis by $[Cu_2(T_2\text{-}p\text{-}X)(H_2O)_4]^{4+}$ derived from **1** and also by $[Cu_2(T_2\text{-}o\text{-}XAc_2)(H_2O)_2]^{2+}$ (**5**). Our results do indicate that a study of the ability of $[Cu_2(T_2\text{-}o\text{-}X)(H_2O)_4]^{4+}$ to cleave such biological fragments is warranted.

Table 4. Rate Constants for the Hydrolysis of BNPP to NPP by Various Copper(II) Complexes Measured at pH 7.4 ([BNPP] = 0.15 mM; [Complex] = 1.7 mM; Ionic Strength = 0.15 M; $T = 323$ K)

complex	$10^7 k$ (s^{-1})
$[Cu_2(T_2\text{-}o\text{-}X)(H_2O)_4]^{4+}$ (**1**)	52
$[Cu_2(T_2\text{-}m\text{-}X)(H_2O)_4]^{4+}$ (**2**)	8.6
$[Cu_2(T_2\text{-}m\text{-}XAc_2)(H_2O)_2]^{2+}$ (**6**)	2.1
$[Cu(tacn)(H_2O)_2]^{2+}$	2.5
$[Cu(Me_3tacn)(H_2O)_2]^{2+}$	630
$[Cu(Me_3tacn)(H_2O)_2]^{2+}$	12[a]
$[Cu(^iPr_3tacn)(H_2O)_2]^{2+}$	430[b]

[a] Rate constant for the hydrolysis of NPP (4-nitrophenyl phosphate). [b] Calculated from the initial rate constants reported by Burstyn and coworkers[50] for the following conditions: [BNPP] = 1.0 mM; [complex] = 0.20 mM; ionic strength = 0.10 M; pH = 7.2 (50 mM HEPES); $T = 323$ K.

One explanation for the greater reactivity of $[Cu_2T_2\text{-}o\text{-}X(H_2O)_4]^{4+}$ relative to $[Cu_2T_2\text{-}m\text{-}X(H_2O)_4]^{4+}$ is that for the latter a bis(hydroxo)-bridged binuclear complex, such as the structurally authenticated $[Cu_2(T_2\text{-}m\text{-}X)(OH)_2]^{2+}$ complex,[28] forms around neutral pH and reduces the "effective" concentration of the cleaving agent. In this context, the crystallization of the *p*-nitrophenyl phosphate hydroxo-bridged complex, $[Cu_2(T_2\text{-}m\text{-}X)(NPP)(\mu\text{-}OH)]^+$ (**4**), in a solution used to measure the rate of cleavage of NPP by $[Cu_2(T_2\text{-}m\text{-}X)(OH_2)_2]^{4+}$ is also instructive in that it highlights the potential for forming complexes bridged by phosphate moieties in solutions used to conduct kinetic studies. In the case of $[Cu_2(T_2\text{-}o\text{-}X)(H_2O)_4]^{4+}$, formation of a similarly inactive complex may be restricted by shortness of the bridge connecting the tacn compartments (4 C's vs 5 in *m*-xylyl). This complex, however, could rearrange in solution forming the inactive sandwich complex, $[Cu(T_2\text{-}o\text{-}X)]^{2+}$. The complex of the bis(tetradentate) $T_2\text{-}m\text{-}XAc_2$ ligand, $[Cu_2(T_2\text{-}m\text{-}XAc_2)(H_2O)_2](ClO_4)_2\cdot 4H_2O$ (**6**), was found to be a poorer BNPP cleavage agent exhibiting a rate of BNPP cleavage that is similar to that of $[Cu(tacn)(OH_2)_2]^{2+}$. Even though the formation of inactive hydroxo-bridged complexes is less likely when such a ligand is coordinated to copper, the copper coordination sphere may be too saturated with strongly binding donor groups for cleavage to be effective.

Our exploratory study of the Cu(II)−Me_3tacn complex revealed a substantial increase in the rate of BNPP cleavage relative to the parent tacn complex. Similar rate enhancements have been reported very recently for the Cu(II)−$^iPr_3$-

(45) Thompson, L. K.; Lee, F. L.; Gabe, E. J. *Inorg. Chem.* **1988**, *27*, 39.
(46) Haddad, M. S.; Wilson, S. C.; Hodgson, D. J.; Hendrickson, D. N. *J. Am. Chem. Soc.* **1981**, *103*, 384.
(47) Kimura, E.; Kodama, Y.; Koike, T.; Shiro, M. *J. Am. Chem. Soc.* **1995**, *117*, 8304.
(48) Deal, K. A.; Burstyn, J. N. *Inorg. Chem.* **1996**, *35*, 2792.
(49) Bencini, A.; Berni, E.; Bianchi, A.; Fedi, V.; Giorgi, C.; Paoletti, P.; Valtancoli, B. *Inorg. Chem.* **1999**, *38*, 6323.

tacn complex.[50] These enhancements of 200-fold that results from N-alkylation of tacn cannot be explained in terms of differences in the acidity leading to increases in the concentration of the hydrolytically "active" $[Cu(L)(OH)(H_2O)]^+$. As for the binuclear complexes, the origins of these differences in reactivity may lie in a lowering of the stability of the "inactive" bis(hydroxo) complexes. The rate of NPP cleavage by $[Cu(Me_3tacn)(H_2O)_2]^{2+}$, obtained from the analysis of the biphasic kinetic data, indicates that this complex is also an effective cleavage agent for phosphate monoesters albeit at a rate that is ca. 50-fold slower than for BNPP. Such differences in the rate of cleavage of diesters and monoesters have been reported previously, but the rates of monoester cleavage are usually slower than found here for $[Cu(Me_3tacn)(H_2O)_2]^{2+}$.[51,52]

Experimental Section

Materials. All chemicals were of reagent grade quality or better, obtained from commercial suppliers and used without further purification. Literature procedures were used to obtain the hexahydrochloride salts of the $(tacn)_2$ ligands (T_2-*o*-X, T_2-*m*-X, and T_2-*p*-X),[53] and the bis(acetate) $(tacn)_2$ ligands (T_2-*o*-XAc_2 and T_2-*m*-X).[54] $[Cu(Me_3tacn)(H_2O)_2](ClO_4)_2$ was prepared from freshly distilled Me_3tacn and copper(II) perchlorate hexahydrate. Solvents were used as received or dried over 4 Å molecular sieves. Distilled water was used throughout.

Physical Measurements. Infrared spectra were recorded using KBr disks on a Perkin-Elmer 1600 series FTIR spectrophotometer. Solution and diffuse reflectance UV−visible−NIR spectra were measured on a Cary 5G spectrophotometer. The instrument used to measure room-temperature magnetic moments was based on a design described elsewhere.[55] Variable-temperature magnetic susceptibilities were measured in a field of 10 000 G (1 T), using a Quantum Design MPMS Squid magnetometer, as described previously.[56] Fitting of the data employed a nonlinear least-squares program called POLYMER written at Monash University. Electron microprobe analyses were made on a JEOL JSM-1 scanning electron microscope through an NEC X-ray detector and pulse-processing system connected to a Packard multichannel analyzer. CHN analyses were performed by either CMAS Pty Ltd., Melbourne, Australia, or the Campbell Microanalytical Services, University of Otago, Dunedin, NZ. ESR spectra were recorded at 77 K on a Varian E12 spectrometer operating at the X-band frequency (9.1 GHz). Solution conductivity measurements were made using a Crison 522 conductimeter with Pt black electrodes. Electrospray mass spectra were recorded on Micromass Platform quadrupole mass spectrometer fitted with an electrospray source or a Bruker BioApex 47e Fourier transform mass spectrometer with a 4.7 T superconducting magnet and an Analytica electrospray source.

Caution! *Although no problems were encountered in this work, metal perchlorate complexes are potentially explosive. They should be prepared in small quantities and handled with care.*

Synthesis of Complexes. ***[Cu$_2$(T$_2$-o-X)Cl$_4$] (1).*** T_2-*o*-X·6HCl (0.50 g, 0.90 mmol) was dissolved in water (10 mL), and a solution of $CuCl_2 \cdot 2H_2O$ (0.61 g, 3.6 mmol dissolved in 10 mL water) was added. The pH of the dark blue solution was adjusted to 7 with 2 M NaOH. The precipitated $Cu(OH)_2$ was removed and the solution heated to reduce the volume by approximately half. The solution was allowed to cool and then left to slowly evaporate. After 2 weeks a small number of blue crystals had formed and were collected by vacuum filtration. Yield: 0.15 g (27%).

Anal. Found: C, 37.9; H, 5.9; N, 13.2. Calcd for $Cu_2C_{20}H_{36}N_6Cl_4$: C, 38.2; H, 5.8; N, 13.4. UV−vis spectrum: solid (λ_{max}, nm) 330, 636, 1043; solution (H_2O; λ_{max}, nm (ϵ, M^{-1} cm^{-1})) 255 (5340), 649 (81), 1028 (39). IR spectrum (KBr; ν, cm^{-1}): 3417 s, 3225 s, 2905 m, 2849 m, 1638 w, 1619 w, 1561 w, 1488 m, 1446 m, 1385 w, 1356 w, 1285 w, 1233 w, 1198 w, 1150 w, 1095 m, 1012 m, 993 w, 944 w, 893 w, 862 w, 833 w, 775 w, 731 w, 656 m, 633 w, 580 w. Electron microprobe: Cu, Cl present. Magnetic moment: μ_{eff} (per Cu) = 1.63 μ_B at 295 K. ESR spectrum (H_2O/ethylene glycol): $g_{||} = 2.29$, $A_{||} = 165 \times 10^{-4}$ cm^{-1}; $g_\perp = 2.06$.

[Cu$_2$(T$_2$-m-X)(H$_2$O)$_4$](ClO$_4$)$_4$·3H$_2$O·NaClO$_4$ (2). T_2-*m*-X·6HCl (0.50 g, 0.90 mmol) was dissolved in water (10 mL), and a solution of $Cu(ClO_4)_2 \cdot 6H_2O$ (1.33 g, 3.60 mmol (excess)) in water (10 mL) was added. The pH of the dark blue solution was adjusted to 7 with 1 M NaOH. The precipitated $Cu(OH)_2$ was removed by filtration and the filtrate loaded onto a Sephadex SP C25 cation-exchange column. The complex was eluted with 0.1 M $NaClO_4$. Two bands separated on the column, the first due to excess Cu(II). The second band was collected and reduced in volume to about 20 mL, and the solution was left to slowly evaporate. After several days a blue powder formed and was collected by vacuum filtration and washed with a small amount of acetone. Yield: 0.34 g (33%).

Anal. Found: C, 21.2; H, 4.3; N, 7.4. Calcd for $Cu_2C_{20}H_{49}N_6O_{27}Cl_5Na$: C, 21.2; H, 4.4; N, 7.4. UV−visible−NIR spectrum: solid (λ_{max}, nm) 305, 640, 1072; solution (H_2O; λ_{max}, nm (ϵ, M^{-1} cm^{-1})) 250 (7780), 644 (72), 1043 (38). IR spectrum (KBr; ν, cm^{-1}): 3424 s br, 3306 m, 2940 m, 2880, 1638 m, 1544 m, 1491 m, 1459 m, 1362 m, 1285 w, 1239 w, 1086 vs, 948 m, 860 w, 826 m, 737 w, 625 s, 582 w, 500 w. Electron microprobe: Cu, Cl, Na present. Magnetic moment: μ_{eff} (per Cu) = 1.85 μ_B at 295 K. ESR spectrum (H_2O/ethylene glycol): $g_{||} = 2.29$, $A_{||} = 170 \times 10^{-4}$ cm^{-1}; $g_\perp = 2.05$.

(50) Deck, K. M.; Tseng, T. A.; Burstyn, J. N. *Inorg. Chem.* **2002**, *41*, 669.
(51) Gómez-Tagle, P.; Yatsimirsky, A. K. *J. Chem. Soc., Dalton Trans.* **2001**, 2663.
(52) Burstyn, J. N.; Deal K. A. *Inorg. Chem.* **1993**, *32*, 3585.
(53) Farrugia, L. J.; Lovatt, P. A.; Peacock, R. D. *J. Chem. Soc., Dalton Trans.* **1997**, 911. Graham, B.; Fallon, G. D.; Hearn, M. T. W.; Hockless, D. C. R.; Lazarev, G.; Spiccia, L. *Inorg. Chem.* **1997**, *36*, 6366.
(54) Fry, F. H.;. Fallon G. D.; Spiccia, L. *Inorg. Chim. Acta* **2003**, *346*, 57.
(55) Hill, J. C. *J. Sci. Instrum.* **1968**, *1*, 52.
(56) Van Langenberg, K.; Batten, S. R.; Berry, K. J.; Hockless, D. C. R.; Moubaraki, B.; Murray, K. S. *Inorg. Chem.* **1997**, *36*, 5006.

$[Cu_2(T_2\text{-}p\text{-}X)Cl_4]$ (3). Dark blue crystals of **3** were obtained from T_2-*p*-X·6HCl (0.50 g, 0.90 mmol) and $CuCl_2$ (0.61 g, 3.6 mmol) using the procedure described for compound **1**. Yield: 0.19 g (33%).

Anal. Found: C, 37.6; H, 5.9; N, 13.4. Calcd for $Cu_2C_{20}H_{36}N_6Cl_4$: C, 38.2; H, 5.8; N, 13.4. UV−visible−NIR spectrum: solid (λ_{max}, nm) 326, 636, 981; solution (H_2O; λ_{max}, nm (ϵ, M^{-1} cm^{-1})) 253 (sh) (5900), 644 (80), 1054 (41). IR spectrum (KBr; ν, cm^{-1}): 3450 br m, 3270 s, 2943 m, 2846 m, 1638 w, 1492 w, 1459 m, 1380 w, 1347 m, 1282 w, 1099 m, 1004 s, 946 m, 894 m, 864 m, 829 m, 766 w, 732 w, 629 m, 581 w. Electron microprobe: Cu, Cl present. Magnetic moment: μ_{eff} (per Cu) = 1.73 μ_B at 297 K. ESR spectrum (H_2O/ethylene glycol): $g_{||} = 2.30$, $A_{||} = 176 \times 10^{-4}$ cm^{-1}; $g_{\perp} = 2.06$.

$[Cu_2(T_2\text{-}m\text{-}X)(NPP)(\mu\text{-}OH)](ClO_4)\cdot H_2O$ (4). Blue crystals of **4** were grown in a solution used to conduct a kinetic run. The solution was ca. 3 mL in volume and consisted of $[Cu_2(T_2\text{-}m\text{-}X)(H_2O)_4](ClO_4)_4\cdot 3H_2O\cdot NaClO_4$ (**2**) (4 mM), Na_2-NPP (5 mM), HEPES buffer (50 mM) at pH 7.4, and $NaClO_4$ (0.04 mM). The solution was kept at 38 °C overnight, after which dark blue needles suitable for crystallographic analysis were collected and washed with water. Yield: 7.1 mg (ca. 70%).

Anal. Found: C, 37.1; H, 5.2; N, 11.6. Calcd for $Cu_2C_{26}H_{43}N_7O_{12}ClP$: C, 37.2; H, 5.2; N, 11.7. UV−visible−NIR spectrum: solid (λ_{max}, nm) 336, 620, ∼950 (sh); solution (DMF; λ_{max}, nm (ϵ, M^{-1} cm^{-1})) 315 (12 500), 674 (166), 1000 (sh). IR spectrum (KBr; ν, cm^{-1}): 3573 m, 3452 m, 3313 m, 3209 m, 2938 m, 2834 m, 1606 m, 1589 m, 1518 s, 1491 m 1459 m, 1346 s, 1242 s, 1133 vs, 1098 vs, 1024 w, 992 s, 952 m, 882 s, 829 m, 752 m, 726 m, 700 w, 624 m, 584 m, 535 m. Electron microprobe: Cu, Cl, P present. Magnetic moment: 0.82 μ_B at 298 K.

$[Cu_2(T_2\text{-}o\text{-}XAc_2)(H_2O)_2](ClO_4)_2\cdot 4H_2O$ (5). The crude oil of T_2-*o*-XAc_2·6HCl was used directly in the synthesis of the copper complex. T_2-*o*-XAc_2 (0.72 g, 1.0 mmol) was dissolved in water (20 mL), and an aqueous solution of $CuCl_2\cdot 2H_2O$ (2.24 g, 13.1 mmol, in excess) was added resulting in a dark blue solution. The pH was adjusted to 5 with 2 M NaOH, and the $Cu(OH)_2$ which formed was removed. The resulting solution was diluted to 2 L with water and loaded onto a Sephadex SP-C25 cation exchange column (2.5 × 25 cm). Addition of 0.1 M $NaClO_4$ eluted several pale blue bands followed by the main band containing the desired complex. The eluent containing the complex was reduced in volume in vacuo to ∼30 mL and left to slowly evaporate. A blue powder formed the following day and was collected by vacuum filtration and washed with MeOH. The blue product was left to air-dry. Yield: 0.31 g (32%).

Anal. Found: C, 30.6; H, 5.0; N, 8.9. Calcd for $Cu_2C_{24}H_{54}N_6O_{20}Cl_2$: C, 30.5; H, 5.8; N, 8.9. UV−visible−NIR spectrum: solid (λ_{max}, nm) 276, 658, 1016; solution (H_2O; λ_{max}, nm (ϵ, M^{-1} cm^{-1})) 257 (6920), 663 (173), 939 (67). IR spectrum (KBr; ν, cm^{-1}): 3420 m, 3297 m, 2928 m, 1598 s, 1494 m, 1437 w, 1400 m, 1370 m, 1318 w, 1099 s, 929 m, 870 w, 832 w, 784 m, 732 m, 624 s. Electron microprobe: Cu, Cl present only. Magnetic moment: μ_{eff} (per Cu) = 1.81 μ_B at 298 K. ESR spectrum (DMF/toluene): $g_{||} = 2.27$, $A_{||} = 166 \times 10^{-4}$ cm^{-1}; $g_{\perp} = 2.05$. Molar conductivity (H_2O): 284 S cm^2 mol^{-1}. Electrospray mass spectrum (H_2O/CH_3CN): *m*/*z* 701 (6%), $[Cu_2(T_2\text{-}o\text{-}XAc_2)]ClO_4^+$.

$[Cu_2(T_2\text{-}m\text{-}XAc_2)(H_2O)_2](ClO_4)_2\cdot 4H_2O$ (6). Compound **6** was prepared in an manner identical with that for **5** using T_2-*m*-XAc_2·6HCl (1.3 g, 1.8 mmol) and $CuCl_2\cdot 2H_2O$ (1 g, 6 mmol excess). The blue powder was collected, washed with MeOH, and air-dried. Yield: 0.66 g (39%).

Anal. Found: C, 31.7; H, 4.9; N, 9.4. Calcd for $Cu_2C_{24}H_{50}N_6O_{18}Cl_2$: C, 31.7; H, 5.6; N, 9.3. UV−visible−NIR spectrum: solid (λ_{max}, nm) 310, 670, 1018; solution (H_2O; λ_{max}, nm (ϵ, M^{-1} cm^{-1})) 670 (166), 1010 (58). IR spectrum (KBr; ν, cm^{-1}): 3424 br s, 3316 m, 2930 m, 2883 w, 1624 s, 1491 w, 1457 w, 1373 m, 1320 w, 1090 s, 1000 m, 931 w, 822 w, 736 w 625 s, 481 w. Electron microprobe: Cu, Cl present. Magnetic moment: μ_{eff} (per Cu) = 1.84 μ_B at 20 °C. ESR spectrum (DMF/toluene): $g_{||} = 2.27$, $A_{||} = 175 \times 10^{-4}$ cm^{-1}; $g_{\perp} = 2.06$. Molar conductivity (H_2O): 340 S cm^2 mol^{-1}. Electrospray mass spectrum (H_2O/CH_3CN): *m*/*z* 701 (13%), $[Cu_2(T_2\text{-}m\text{-}XAc_2)]ClO_4^+$.

X-ray Crystallography. Data were collected for a blue crystal of $[Cu_2(T_2\text{-}p\text{-}X)Cl_4]$ (**3**), 0.05 × 0.32 × 0.32 mm, by employing graphite-monochromatized MoKα radiation, λ = 0.710 73 Å, on a Rigaku AFC6R diffractometer. Corrections were made for Lorentz and polarization effects[57] and for absorption using an empirical procedure (DIFABS[58]). The structure was solved by direct methods[59] and refined by a full-matrix least-squares procedure based on *F*.[57] Non-hydrogen atoms were refined anisotropically, and hydrogen atoms were included in the model in their calculated positions. The refinement was continued until convergence with the application of a weighting scheme of the form $w = 1/[\sigma^2(F_o)^2 + 0.00005|F_o|^2]$.

Intensity data for a blue crystal of $[Cu_2(T_2\text{-}m\text{-}X)(NPP)(\mu\text{-}OH)](ClO_4)\cdot H_2O$ (**4**) of approximate dimensions 0.2 × 0.2 × 0.2 mm were measured on a Nonius Kappa CCD diffractometer using graphite-monochromated Mo Kα radiation (λ = 0.710 73 Å). Data, collected to a maximum 2θ value of 60.0°, were processed and corrected for Lorentz and polarization effects using Nonius software.[60] The structure was solved by direct methods and refined by full-matrix least squares on F^2 using the SHELX-97 program suite.[61] Non-hydrogen atoms were refined anisotropically. The C−H and N−H hydrogen atoms were included in calculated positions with isotropic thermal parameters fixed at 1.2 times that of the respective carbon or nitrogen atom. The O−H hydrogen atoms were, however, located from difference maps and refined subject to distance restraints (DFIX 0.84) with

(57) *teXsan*: *Structure Analysis Software*; Molecular Structure Corp.: The Woodlands, TX, 1997.
(58) Walker, N.; Stuart, D. *Acta Crystallogr., Sect. A* **1983**, *39*, 158.
(59) Altomare, G.; Cascarano, G.; Giacovazzo, C.; Guagliardi, A.; Burla, M. C.; Polidori, G.; Camalli, M. *J. Appl. Crystallogr.* **1994**, *27*, 435.
(60) (a) Hooft, R. *COLLECT Software*; Nonius BV: Delft, The Netherlands, 1998. (b) Otwinowski, Z.; Minor, W. In *Methods in Enzymology*; Carter, C. W., Sweet, R. M., Eds.; Academic Press: New York, 1996.
(61) Sheldrick, G. M. *SHELX-97*; University of Göttingen: Göttingen, Germany, 1997.

Table 5. Crystal Data for **3** and **4**

	3	**4**
chem formula	$C_{20}H_{36}Cl_4Cu_2N_6$	$C_{26}H_{43}Cu_2N_7O_{12}ClP$
M_r	629.45	839.17
cryst system	orthorhombic	orthorhombic
space group	Pbca	Pbcn
temp (K)	293	123
a, Å	13.11(2)	22.994(5)
b, Å	30.139(10)	14.192(3)
c, Å	7.28(1)	20.833(4)
V, Å^3	2879(5)	6798(2)
Z	4 (dimers)	8
D_c, g cm^{-3}	1.452	1.640
μ(Mo Kα), cm^{-1}	18.67	14.48
no. of data measd	3850	62 384
no. of unique data	3849	9582
no. of obsd data	1088, $I \geq 3\sigma(I)$	5819, $I \geq 2\sigma(I)$
no. of params	145	451
R[a]	0.059	0.066
R_w	0.054[b]	0.113[c]
residual ρ, e Å^{-3}	0.55	0.86

[a] $R = \Sigma||F_o| - |F_c||/\Sigma|F_o|$. [b] $R_w = [\Sigma w(|F_o| - |F_c|)^2/\Sigma w(F_o)^2]^{1/2}$. [c] $R_w = [\Sigma w(F_o^2 - F_c^2)^2/\Sigma w(F_o^2)^2]^{1/2}$.

thermal parameters fixed at 1.5 times that of the respective oxygen atom.

Crystal data and refinement details are summarized in Table 5. The numbering schemes, shown in Figures 2a and 3a, were drawn with ORTEP[62] for 50% displacement ellipsoids.

Kinetic Studies. Reaction mixtures for use in kinetic studies were prepared by mixing equal volumes of the Cu(II) complexes (5.1 mM solution at $I = 0.225$ M ($NaClO_4$)), HEPES buffer (150 mM solution, $I = 0.225$ M ($NaClO_4$)), and BNPP (0.045 mM). This gave solutions with final concentrations of 1.7 mM in complex, 0.15 mM in BNPP, and 50 mM in HEPES buffer at pH 7.4 (at 50 °C) and $I = 0.15$ M. Following mixing of the solutions, the temperature was allowed to equilibrate at 50 °C for several minutes before readings commenced. Reactions were monitored on a Cary 5G UV−visible−NIR spectrophotometer by measuring the release of *p*-nitrophenylate from BNPP at 400 nm ($\epsilon = 11\,800$ M^{-1} cm^{-1} at pH 7.4). The reaction mixtures were maintained at 50 °C by a heated temperature block. Absorbance readings were taken every 10 min for periods of up to 8000 min. The analysis of data for the cleavage of BNPP by $[Cu(Me_3tacn)(OH_2)_2]^{2+}$ was carried out using the double-exponential equation:

$$\text{abs} = A + Be^{-k_{obs1}t} + Ce^{-k_{obs2}t} \quad (2)$$

The raw data was transposed and fitted to eq 2 to determine k_{obs1} and k_{obs2}, where k_{obs1} = rate of production of the first mole of *p*-nitrophenylate (NP) from BNPP and k_{obs2} = rate of production of the second NP ion from NPP formed by the cleavage of BNPP. The number of moles of *p*-nitrophenylate released per/mol of BNPP was calculated using the molar extinction coefficient of this ion at 400 nm and pH = 7.4 and confirmed the release of 2 mol on NP at the end of the reaction. For all other complexes, the rate constants were determined using the initial rates method.[50]

Acknowledgment. This work was supported by the Australian Research Council. F.H.F. and P.J. were the recipients of an Australian Postgraduate Award and a Monash Graduate Scholarship, respectively. We thank Dr. Simon Drew for conducting the ESR measurements and one of the reviewers for bringing ref 34 to our attention.

Supporting Information Available: Crystallographic files in CIF format. This material is available free of charge via the Internet http://pubs.acs.org.

IC0342595

(62) Johnson, C. K. *ORTEP*; Report ORNL-5138; Oak Ridge National Laboratory: Oak Ridge, TN, 1976.